
Dossier

*This paper is a part of the hereunder thematic dossier published in OGST Journal, Vol. 69, No. 5, pp. 773-969 and available online here*

Cet article fait partie du dossier thématique ci-dessous publié dans la revue OGST, Vol. 69, n°5, pp. 773-969 et téléchargeable ici

DOSSIER Edited by/Sous la direction de : **P.-L. Carrette**

# *PART 1*
# *Post Combustion $CO_2$ Capture*
# Captage de $CO_2$ en postcombustion

*Oil & Gas Science and Technology – Rev. IFP Energies nouvelles*, Vol. 69 (2014), No. 5, pp. 773-969

*Oil & Gas Science and Technology – Rev. IFP Energies nouvelles*, Vol. 69 (2014), No. 5, pp. 833-849

DOI: 10.2516/ogst/2013144

Dossier

*Post Combustion $CO_2$ Capture*
Captage de $CO_2$ en postcombustion

# Equilibrium and Transport Properties of Primary, Secondary and Tertiary Amines by Molecular Simulation

Gustavo A. Orozco[1,2], Carlos Nieto-Draghi[1], Allan D. Mackie[2] and Véronique Lachet[1]*

[1] *IFP Energies nouvelles, 1-4 avenue de Bois-Préau, 92852 Rueil-Malmaison - France*
[2] *Departament d'Enginyeria Quimica, ETSEQ, Universitat Rovira i Virgili, Av. dels Pa sos Catalans 26, 43007 Tarragona - Spain*
*e-mail: veronique.lachet@ifpen.fr*

* Corresponding author

**Résumé — Propriétés d'équilibre et de transport d'amines primaires, secondaires et tertiaires par simulation moléculaire** — Grâce à la mise en œuvre de techniques de simulation moléculaire telles que le Monte-Carlo et la dynamique moléculaire, nous présentons ici différents résultats de simulation de propriétés thermodynamiques et de transport pour des amines primaires, secondaires et tertiaires. Ces calculs utilisent pour représenter les amines un champ de force récemment proposé basé sur l'approche des Atomes Unifiés Anisotropes (AUA). Différentes amines ont été ainsi étudiées, parmi lesquelles la *n*-ButylAmine (amine primaire), la di-*n*-ButylAmine (amine secondaire), la tri-*n*-ButylAmine (amine tertiaire) et la 1,4-ButaneDiAmine (multi-amine). Des simulations conduites dans l'ensemble isotherme-isobare (NPT) nous ont permis d'accéder aux propriétés de transport (coefficients de viscosité) de ces molécules en fonction de la température. Nous avons également étudié différentes propriétés d'équilibre de ces mêmes constituants (diagrammes de phase liquide-vapeur, enthalpies de vaporisation, pressions de vapeur saturante, températures d'ébullition, températures et densités critiques) grâce à la mise en œuvre de calculs Monte-Carlo dans l'ensemble de Gibbs NVT. Nous avons aussi calculé les enthalpies d'excès des mélanges eau-*n*-ButylAmine et *n*-heptane-*n*-ButylAmine par simulation Monte-Carlo NPT. Nous présentons également des calculs de tensions superficielles de la *n*-ButylAmine et des fonctions de distribution radiale. Enfin, nous nous sommes intéressés aux constantes de Henry physiques du protoxyde d'azote ($N_2O$) et de l'azote ($N_2$) dans des solutions aqueuses de *n*-ButylAmine. D'une manière générale, nous avons obtenu un bon accord entre les informations expérimentales disponibles et nos résultats de simulation pour l'ensemble des propriétés étudiées, témoignant de la capacité de prédiction du champs de force AUA pour les amines.

***Abstract* — *Equilibrium and Transport Properties of Primary, Secondary and Tertiary Amines by Molecular Simulation*** — *Using molecular simulation techniques such as Monte-Carlo (MC) and molecular dynamics (MD), we present several simulation results of thermodynamic and transport properties for primary, secondary and tertiary amines. These calculations are based on a recently proposed force field for amines that follows the Anisotropic United Atom approach (AUA). Different amine molecules have been studied, including* n-*ButylAmine, di-*n-*ButylAmine, tri-*n-*ButylAmine and 1,4-ButaneDiAmine for primary, secondary, tertiary and multi-functional amines respectively. For the transport properties, we have calculated the viscosity coefficients as a function of temperature*

*using the isothermal-isobaric (NPT) ensemble. In the case of the pure components, we have investigated different thermodynamic properties using NVT Gibbs ensemble simulations such as liquid-vapor phase equilibrium diagrams, vaporization enthalpies, vapor pressures, normal boiling points, critical temperatures and critical densities. We have also calculated the excess enthalpies for water-*n*-ButylAmine and* n*-heptane-*n*-ButylAmine mixtures using Monte-Carlo simulations in the NPT ensemble. In addition, we present the calculation of liquid-vapor surface tensions of* n*-ButylAmine using a two-phase NVT simulation as well as the radial distribution functions. Finally, we have investigated the physical Henry constants of nitrous oxide ($N_2O$) and nitrogen ($N_2$) in an aqueous solutions of* n*-ButylAmine. In general, we found a good agreement between the available experimental information and our simulation results for all the studied properties, ratifying the predictive capability of the AUA force field for amines.*

## INTRODUCTION

World energy consumption is constantly increasing and is primarily based on fossil fuels such as oil, coal and gas. However, besides being one of the main energy sources, they are also considered to be the foremost cause for so-called greenhouse gas emissions and subsequently global warming. Nowadays, many efforts are directed at reducing these greenhouse gas emissions and $CO_2$ capture and storage processes are of particular interest. Different technological alternatives have been proposed where the most widely accepted are pre-combustion, oxyfuel combustion and post-combustion processes. Pre-combustion involves removal of $CO_2$ prior to combustion, to produce hydrogen. Unlike the classical combustion process, where air is used as the oxygen source, in the oxyfuel process the combustion is carried out using pure oxygen. In pre-combustion capture, the carbon present in the fuel is separated. Finally, in the post-combustion process, the effluent gas stream is treated with an aqueous solution of amines where the carbon dioxide is physcially and chemically absorbed.

Different solvents have been proposed as candidates for such a process based on experimental results. However, a detailed microscopic understanding of the manner in which these systems behave is not available at present. Such a microscopic vision is essential in order to be able to improve and optimize these processes in a systemic way. Here, molecular simulation can play a key role in elucidating the molecular mechanisms. Despite the fact that experiments are per se irreplaceable, many advantages of molecular simulation can be mentioned. Among them is the possibility to avoid the uncertainties produced by uncontrolled external factors therefore allowing the system to be analyzed under specific and well defined situations. It is also possible either to simulate the systems under extreme conditions, for instance at high pressures, temperatures, in toxic environments, or to carry out simulations of hazardous materials or very expensive or even hypothetical substances.

The main requirement to obtain accurate predictions from molecular simulations is to have a force field able to reproduce different properties at different conditions with a reduced set of parameters. When the same set of force field parameters can be applied without any modification for different molecules and for different properties, we define the force field as being transferable. In general, a force field can be considered as an empirical approximation that tries to represent the total energy of a set of molecules from a classical point of view. More details about force fields will be discussed later on.

For some time now, IFP Energies nouvelles has developed transferable force fields based on the Anisotropic United Atom (AUA) approach. The first AUA force field was proposed and applied by Toxvaerd [1] for hydrocarbons. Later on, this force field was improved and reparameterized by Ungerer *et al.* [2] in a force field known as AUA4. The AUA4 force field for hydrocarbons has been extended to additional chemical groups. Parameters have subsequently been developed for functional groups such as sulfides and thiols [3], cyclic alkanes [5], olefins [4], benzene and styrene [6], polyaromatics and napthenoaromatics [7], aromatic hydrocarbons including electrostatic interactions [8], thiophenes [9], alcohols and polyalcohols [10, 11], polycyclic aromatics [12], ketones and aldehydes [13], ethers and glycol ethers [14], carboxylate esters [15] and recently for primary, secondary and tertiary amines [16, 17]. This extension of the AUA4 force field is the model that has been used in this present work. It is important to point out that, along with the AUA approach, there also exist additional transferable force field approaches, namely:

- All Atom (AA), where all the atoms belonging to the molecule are taken into account with a force center for each atom;
- United Atom (UA), where only one force center per functional group is considered, this force center being located at the center of the main atom of the group.

Apart from the AUA4 force field for amines, other molecular models to study this family of molecules have been proposed. For example, Rizzo and Jorgensen [18] and Wick *et al.* [19] proposed the OPLS-AA (Optimized Potential for Liquid Simulations - All Atom) and the TraPPE-EH (Transferable Potential for Phase Equilibria Explicit Hydrogens) respectively, both of them being based on the all atom approach. Additional attempts to model some specific amine molecules without explicitly considering transferability can also be found in the literature. A detailed discussion of the available molecular simulation works on amines proposed in the literature can be found in references [16] and [17]. It is worth mentioning that a previous AUA4 force field was proposed by Boutard *et al.* [20] in 2005 to model primary amines. In their work, a different set of charges was proposed for each of the three studied amines, obtaining average deviations between calculated and experimental values around 4-6% for liquid densities and 40-60% for vapor pressures.

In this work, our new AUA4 force field for amines [16, 17] will be applied to predict the behavior of different amine molecules. Up to now, the transferability of our force field has been checked for 20 different amines including linear and branched molecules. Furthermore, the transferability toward multifunctional amines including highly complex molecules such as DiEthyleneTriAmine (DETA) has also been studied obtaining very good accuracy. In addition, there are no restrictions in our force field towards including more molecules and therefore the study can be extended to an even bigger set of molecules thanks to the different torsional potentials that have been fitted. So far, the main contributions of our AUA4 force field for amines can be summarized as follows: firstly, its ability to accurately predict both thermodynamic and transport properties at the same time; secondly, it has been tested on a big set of different molecules including different structures without the limitation to linear chains; thirdly, the model allows us to study important industrial applications such as $CO_2$ capture and natural gas sweetening processes. However it is not restricted to these two domains and can also be applied to many others because of the wide use of amines in the industry. Finally, considering that our force field is based on the united atom approach, less force centers need to be included compared with the commonly used all atom potentials.

The aim of this contribution is to present the role and power that molecular simulation can play when predicting thermodynamic and transport properties, in particular: surface tensions, excess properties, and Henry constants of gases in an amine aqueous solution. The article is organized as follows. First in Section 1, we present the physical description of our model. Second, the simulation methods used to calculate thermodynamic and transport properties are detailed in Section 2. Then in Section 3, we show the capability of the force field for the estimation of different properties such as densities of coexisting liquid and vapor phases, excess properties, Henry constants, surface tensions, viscosity coefficients and several inter and intra molecular radial distribution functions. Finally, the main conclusions are given.

## 1 FORCE FIELD FEATURES

The AUA4 force field for amines divides as usual the total energy $U$ of the system into two parts made up by bonded and non-bonded interactions as given by Equation (1):

$$U = U_{\text{Bonded}} + U_{\text{Non-bonded}} \tag{1}$$

All bonds are considered to be rigid, so that the bonded energy is again divided into two different contributions given by:

$$U_{\text{Bonded}} = U_{\text{Bending}} + U_{\text{Torsion}} \tag{2}$$

The first term in Equation (2) represents the associated energy with bond angle deformations at small displacements from equilibrium. This energy is known as the bending energy and is expressed as an harmonic potential as a function of the angle $\theta$, which is the angle between two successive bonds:

$$U_{\text{Bending}} = \frac{1}{2} k_{\text{Bending}} (\cos\theta - \cos\theta_{\text{o}})^2 \tag{3}$$

The last term in Equation (2) represents the torsional energy originating from sets of four connected atoms, as a function of the dihedral angle:

$$U_{\text{Torsion}} = \sum_{i=0}^{8} a_i [\cos\chi]^i \tag{4}$$

where the $\chi$ angle has been defined such that $\chi = \phi + 180$, $\phi$ being the dihedral angle and $a_i$ the corresponding Fourier coefficients.

Non-bonded interactions (*Eq. 5*) are represented by contributions from the van der Waals force and the electrostatic force. For the van der Waals interactions, a big variety of potentials is available (*e.g.*, MIE, Buckingham, hard sphere, square well, etc.). We have used in this work the Lennard-Jones (6,12) potential given by Equation (6), where ε is associated with the energy and $\sigma$ the size of the force center:

$$U_{\text{Non-bonded}} = U_{\text{van-Waals}} + U_{\text{Electrostatic}} \quad (5)$$

$$U_{\text{van-Waals}} = 4\epsilon_{ij}\left[\left(\frac{\sigma_{ij}}{r_{ij}}\right)^{12} - \left(\frac{\sigma_{ij}}{r_{ij}}\right)^{6}\right] \quad (6)$$

Besides the proposed molecules, we have also included the study of the nitrogen-nitrogen intramolecular distances for additional multifunctional molecules, namely, 1,2-EthaneDiAmine (EDA) and 1,3-PropaneDiAmine (PDA). For EDA an extra-term representing the 1-4 Lennard-Jones intramolecular interactions is also included.

Electrostatic interactions are calculated *via* a Coulombic force:

$$U_{\text{Electrostatic}} = \frac{q_i q_j}{4\pi\epsilon_0 r_{ij}} \quad (7)$$

where $q_i$ represents the partial charge of the $i$-th force center and $\varepsilon_0$ the vacuum permittivity. For the case of multifunctional amines, intramolecular electrostatic interactions were also considered following the local dipole approach proposed by Ferrando *et al.* [11].

Figure 1 gives a schematic representation of the AUA4 force field for primary, secondary and tertiary amines, using methyl, di-methyl and tri-methylamine as examples. As shown, all amino groups have in common four partial charges (red filled circles) located on the nitrogen and the three neighbor atoms. As usual, explicit hydrogens were considered by way of partial charges and without Lennard-Jones parameters. For the case of the methyl or methylene groups, the force centers are located according to the AUA4 rules for hydrocarbons [21]. The amino group force center is also located according to the AUA rules, namely:

- for primary amines (methylamine in *Fig. 1*), since two hydrogens are present, the force center is located on the bisector of the HNH bending angle at a distance ($\delta$) from the nitrogen;
- for secondary amines, since only one hydrogen is present, the force center is located on the N–H bond at a $\delta$ displacement from the nitrogen atom; and finally;
- for tertiary amines since no hydrogens are present in the amino group, no AUA4 displacement ($\delta$) is required and therefore the force center is located on the nitrogen atom.

We would like to emphasize that our extension of the AUA4 force field for amines is made up of only three new adjustable parameters ($\sigma$, ε and $\delta$), which correspond to the dispersion-repulsion in the case of primary and secondary amines. For tertiary amines, only two new adjustable parameters are needed corresponding to $\sigma$ and ε of the nitrogen atom. The set of partial charges for primary amines corresponds to the TraPPE-EH force field while for secondary and tertiary amines the sets of partial charges have been specially developed for the AUA4 force field and were based on Density Functional Theory (DFT) calculations [16, 17].

Interactions between the different force centers were obtained using the Lorentz-Berthelot combining rules:

$$\epsilon_{ij} = \sqrt{\epsilon_{ii}\epsilon_{jj}} \quad (8)$$

$$\sigma_{ij} = \frac{1}{2}(\sigma_{ii} + \sigma_{jj}) \quad (9)$$

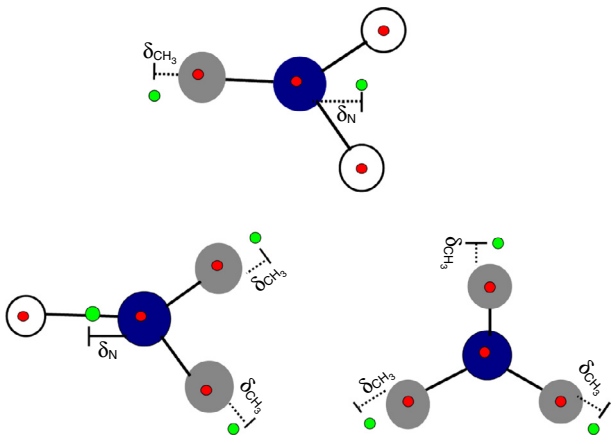


Figure 1

Schematic representation of the AUA4 force field for primary (top), secondary (left) and tertiary (right) amines. Green filled circles represent the Lennard-Jones force centers while red filled circles represent the partial charges.

TABLE 1
Partial charges

| Force center | $q$ (e) | References |
|---|---|---|
| $CH_2$, $CH_3$, CH | +0.180 if bonded to 1° amine | [16] |
| | +0.176 if bonded to 2° amine | [17] |
| | +0.230 if bonded to 3° amine 0 elsewhere | [17] |
| N (1° amine) | −0.892 | [19] |
| N (2° amine) | −0.730 | [17] |
| N (3° amine) | −0.690 | [17] |
| H (1° amine) | +0.356 | [19] |
| H (2° amine) | +0.378 | [17] |

TABLE 2
Non-bonded Lennard-Jones parameters

| Force center | ε (K) | σ (Å) | δ (Å) | References |
|---|---|---|---|---|
| $CH_3$ | 120.15 | 3.607 | 0.216 | [21] |
| $CH_2$ | 86.29 | 3.461 | 0.384 | [21] |
| CH | 50.98 | 3.363 | 0.646 | [21] |
| N (1° amine) | 137.46 | 3.415 | 0.170 | [16] |
| N (2° amine) | 120.66 | 3.172 | 0.497 | [17] |
| N (3° amine) | 47.00 | 2.600 | 0 | [17] |
| H (N) | 0 | 0 | 0 | [16] |

The Lennard-Jones parameters for the amino groups were obtained through a numerical optimization [16] while all the L-J parameters for the hydrocarbons were taken from the AUA4 potential [21]. Tables 1 and 2 summarize the partial charges and the L-J parameters used in our model respectively. Bond lengths and bending angles are given in Tables 3 and 4.

Table 5 shows the torsional potentials used in this work, all of them belong to the AUA4 force field for amines works.

For all the multifunctional molecules studied in this work, it was necessary to calculate the intramolecular electrostatic interactions, using the local dipole approach [11]. This approach was already used in our previous works on primary, secondary and tertiary amines for multifunctional amines such as ethylenediamine and ethylenetriamine, among others. The advantages when using the local dipole approach are basically that neither additional interaction terms nor scaling factors need to be considered.

TABLE 3
Bond lengths

| Bond | $r_0$ (Å) | References |
|---|---|---|
| H–N | 1.010 | [18] |
| C–N[a] | 1.429 | [16] |
| C–N[b] | 1.463 | [22] |
| C–C | 1.535 | [2] |

[a] Value for primary amines.
[b] Value for secondary and tertiary amines.

TABLE 4
Bending parameters

| Angle | $k_{Bending}$ (K) | $\theta_0$ (deg) | References |
|---|---|---|---|
| $CH_x$–N–H | 39 642 | 109.50 | [18] |
| H–N–H | 47 681 | 106.40 | [18] |
| C–C–N | 63 630 | 109.47 | [18] |
| $CH_x$–$CH_2$–$CH_x$ | 74 900 | 114.00 | [2] |
| $CH_x$–CH–$CH_x$ | 72 700 | 112.00 | [2] |
| $CH_x$–NH–$CH_x$ | 57 128 | 112.30 | [22] |
| $CH_x$–N–$CH_x$ | 57 128 | 111.00 | [22] |

## Water Model and Gas Models

In order to include water molecules in our mixtures, we have chosen the TIP4P/2005 model [23]. Many of the non-polarizable water models have been evaluated in a recent review by Vega and Abascal [24]. In this work, different water properties such as dielectric constants, melting properties, phase equilibrium diagrams among others were calculated. They have found that the TIP4P/2005 model corresponds to the one that best predicts on average the water behavior for all these properties. For $N_2O$ and $N_2$, the molecular models proposed by Lachet *et al.* [25] and Delhommelle [26] were chosen respectively.

Table 6 summarizes the force field parameters used for water and for the two studied gases. As can be observed in the table, the $N_2O$ model proposed by Lachet *et al.* [25] is made up of three force centers and three partial charges located on the atoms. In addition, this molecule has a $N_1$-$N_2$-O angle equal to 180 degrees. On the other hand, the model for water is made up of one force center located on the oxygen and three partial charges, two of which are located on the hydrogens and one in a point M which is located on the bisector of the H-O-H angle

TABLE 5
Torsion parameters $a_i$ (K)

| Torsion | $a_0$ | $a_1$ | $a_2$ | $a_3$ | $a_4$ | $a_5$ | $a_6$ | $a_7$ | $a_8$ | References |
|---|---|---|---|---|---|---|---|---|---|---|
| $CH_x$-$CH_2$-N-H | 154.98 | 869.66 | 902.48 | −586.25 | −651.38 | −607.86 | 253.22 | 149.74 | 102.90 | [16] |
| $CH_x$-$CH_2$-NH-$CH_x$ | 134.01 | 1 028.60 | 1 427.94 | −1 739.77 | −960.76 | −106.72 | 693.93 | −177.42 | −170.38 | [17] |
| $CH_x$-$CH_2$-N-$CH_x$ | 189.01 | 979.05 | 1 482.82 | −1 436.82 | −1 465.09 | −1 219.26 | 913.04 | 541.13 | 16.99 | [17] |
| $CH_x$-$CH_2$-$CH_2$-N | 816.65 | 2 509.94 | 9.01 | −3 609.00 | −54.51 | 286.01 | −104.22 | −133.18 | 279.10 | [16] |
| $CH_x$-$CH_2$-$CH_2$-$CH_x$ | 1 001.35 | 2 129.52 | −303.06 | −3 612.27 | 2 226.71 | 1 965.93 | −4 489.34 | −1 736.22 | 2 817.37 | [21] |

TABLE 6
Force field parameters for $N_2O$, water, and $N_2$

| Site | ε (K) | $\sigma$ (Å) | $q$ (e) | Bond length (Å) | References |
|---|---|---|---|---|---|
| $N_1$ ($N_2O$) | 78.107 | 3.116 | −0.3400 | $N_1 - N_2$ = 1.1282 | [25] |
| $N_2$ ($N_2O$) | 34.647 | 2.927 | +0.6800 | $N_2 - O$ = 1.1842 | [25] |
| O ($N_2O$) | 65.891 | 3.044 | −0.3400 | | [25] |
| O ($H_2O$) | 93.2 | 3.1589 | 0.0 | O – H = 0.9572 | [23] |
| H ($H_2O$) | 0.0 | 0.0 | +0.5564 | | [23] |
| M ($H_2O$) | - | - | −1.1128 | | [23] |
| N ($N_2$) | 36.0 | 3.300 | −0.5075 | N – N =1.098 | [26] |
| | | | +1.015 | | [26] |

at a distance of 0.1546 Å from the oxygen. The H-O-H angle of the TIP4P/2005 model corresponds to the experimental one and is equal to 104.52°. Finally, the $N_2$ model is made up of three charges, two located on the nitrogen atoms and one on the mid point of the N–N bond.

## 2 COMPUTATIONAL METHODS

Several different molecular simulation techniques were used in this work. In the following the simulation details as well as the procedure are briefly given. All simulations were performed using the in-house GIBBS Monte-Carlo (MC) code developed by IFPEN and Orsay University [21], except the viscosity coefficients which were calculated using the molecular dynamics code NEWTON developed at Orsay University [27].

### 2.1 Thermodynamic Equilibrium Properties

To calculate the thermodynamic equilibrium properties such as vaporization enthalpies, vapor pressures and liquid densities, Gibbs ensemble MC simulations at constant volume and temperature (NVT) with periodic boundary conditions and the minimum image convention were used [28]. With regards to the L-J interactions between force centers, a spherical cutoff equal to half of the simulation box was applied, while for long-range electrostatic interactions the Ewald procedure was chosen [29] with a maximum of 7 vectors in each direction of reciprocal space and with the scaling parameter $\alpha = 2$ in reduced units.

Configurational phase space was sampled by means of different MC moves, namely, translations (15%), rotations (15%), configurational bias regrowths (15%), internal rotations (15%) (*i.e.* the rotation of a force center around its nearest neighbors), transfers with insertion bias (39.5%) and volume changes (0.5%). The amplitudes of translations, rotations and volume changes were adjusted during the simulation to achieve an acceptance ratio of 40% for these moves.

Most of the simulations were performed using 10 million Monte-Carlo Steps (MCS) for the equilibration part and 80 million MCS for the production part, where one MCS corresponds to a simple MC move.

Nearly all the studied systems contained a total of 300 molecules, except for temperatures close to the critical point, where the size of the system was increased up to 600 molecules.

### 2.2 Molecular Dynamics

Viscosity coefficients were calculated using molecular dynamics. In this case, the equations of motion were integrated by means of the velocity Verlet algorithm with constrained bonds using the Rattle algorithm [30]. The simulations were performed in the NPT ensemble using both the Berendsen barostat and thermostat. Equilibration runs of 1 ns were used while 5 ns were applied for the production part. In both cases, the integration time step was 2 fs. A Verlet nearest neighbor list was also included in order to improve the performances of the simulations. In all cases, 300 molecules were placed in a cubic box with periodic boundary conditions. To estimate the viscosity coefficients, both the Einstein and Green-Kubo formalisms were applied. In order to calculate the viscosity coefficients, four different and independent initial configurations were used, hence the values presented here correspond to the average of the obtained results for the four different configurations together with the corresponding standard deviations.

### 2.3 Excess Enthalpies

Using MC simulations in the NPT ensemble, we have calculated the excess enthalpies of two different systems, namely, *n*-ButylAmine + water and *n*-ButylAmine + *n*-heptane. We have used the same moves as the ones used in the Gibbs ensemble with 300 molecules and a total of 250 million MCS. The aforementioned TIP4P/2005 potential was used as the water model. The excess enthalpies, $H^E$, for a binary system were calculated at each mixture composition by means of Equation (10):

$$H^E = H - x_1 H_1 - (1 - x_1) H_2 \tag{10}$$

with $H$ the enthalpy defined as:

$$H = U_{\text{ext}} + U_{\text{int}} + K + PV \tag{11}$$

where $U_{\text{ext}}$ is the intermolecular potential energy, $U_{\text{int}}$ the internal potential energy, $K$, $P$, $V$ are the total kinetic energy, pressure, volume of the system respectively. $H_i$ is the enthalpy of the pure component $i$ and $x_1$ the molar fraction of component 1. We assume that the kinetic energy of the mixture can be obtained from the mole average of the pure component contributions. Thus, two independent simulations need to be carried out in order to estimate the configurational enthalpies for the pure components $H_1$ and $H_2$. Then, at a fixed composition of the binary mixture, the total configurational enthalpy $H$ can be determined and therefore the corresponding excess enthalpy is calculated from Equation (10). For both mixtures, nine different compositions were calculated ranging between 0.1 and 0.9 in steps of 0.1.

### 2.4 Henry Constants

In order to calculate Henry constants of gases in an aqueous solution of amine, $K_{\text{H}}$, we have performed MC simulations in the isothermal-isobaric ensemble (NPT) at two different temperatures, namely 303 K and 313 K, and atmospheric pressure. For all cases, a simulation of 550 MCS was carried out using the same moves as in the Gibbs ensemble, except transfer moves that have been replaced by test insertion moves. Four hundred molecules (368 water molecules and 32 *n*-ButylAmine molecules) were used, which corresponds to an amine molar fraction of 8%. The so-called Widom particle insertion algorithm was used to calculate the gas chemical potential [29, 31].

The Henry constant ($K_{\text{H}}$) is related to the excess chemical potential ($\mu^E$) by means of Equation (12):

$$\frac{\mu^E}{k_B T} = \ln \frac{K_{\text{H}}}{\rho k_B T} \tag{12}$$

where $k_B$ represents the Boltzmann constant, $T$ the temperature of the system and $\rho$ the density of the solvent.

Thus, if the chemical potential is calculated, then the Henry constant can be directly estimated. According to the Widom particle insertion formula [31], the chemical potential is calculated from an ensemble average (*Eq. 13*):

$$\mu^E = -k_B T \ln \left\langle \frac{PV}{k_B T (N+1)} \exp\left(-\frac{\Delta U}{k_B T}\right) \right\rangle_{NPT} \tag{13}$$

where $\Delta U$ is the potential energy difference due to the insertion of the test molecule, $P$, $N$ and $V$ correspond to the pressure, total number of particles and volume of the system.

### 2.5 Surface Tensions

In order to check the accuracy of the AUA4 force field for amines in predicting interfacial properties, the surface tension $\gamma$ of *n*-ButylAmine has been calculated at different temperatures. The simulations have been carried out in

the NVT ensemble in a rectangular parallelepiped box. We have considered a system with two planar liquid-vapor surfaces lying in the $x$,$y$ plane and the $z$-axis in the direction normal to the surface. Since the geometry of the system has a heterogeneity along the axis normal to the interface ($z$-axis), we calculated the long-range correction to the repulsion-dispersion energy as a function of $z$ by splitting the cell into slabs. The total long-range correction energy, $U_{LRC}$, was then calculated by summing up all the local contributions of each slab. The $U_{LRC}$ term was then included in the total energy of the system to be used in the Metropolis scheme. Tail corrections to the surface tension have also been accounted for using the expressions given by Biscay *et al.* [32]. More detailed descriptions of these models and long-range corrections can be found elsewhere [33-36].

Two different methods have been used to calculate surface tensions. The first one is the Irving-Kirkwood (IK) method [37] based on the mechanical definition of the surface tension. The second method used is the Test-Area (TA) method [38], based upon a thermodynamic route and expressing the surface tension as a change in the free energy for a change in the surface area.

The initial configuration of the system was prepared from equilibrated bulk liquid and bulk vapor phases, the bulk liquid phase being surrounded by two bulk vapor phases along the $z$ direction. The $Lx$ and $Ly$ dimensions of the resulting simulation box were fixed to 40 Å, and the $Lz$ dimension to 300 Å. A total of 789 to 932 molecules were used depending on the temperature. The Ewald sum technique was used to calculate the electrostatic energy, with a number of reciprocal vectors equal to 8 along the $x$ and $y$ axis, and equal to 60 along the $z$ axis. The MC moves and attempt probabilities used during the simulations are: translation (25%), rigid rotation (25%), flip (25%) and configurational-bias regrowth (25%). A typical simulation consists of an equilibration run followed by a production run of around 150 MCS each.

## 3 RESULTS

Using the AUA4 transferable force field for amines, *i.e.* the original parameters without any modifications, we have studied the behavior of one primary amine (*n*-ButylAmine), one secondary amine (di-*n*-ButylAmine), one tertiary amine (tri-*n*-ButylAmine), and one multifunctional amine (1,4-ButaneDiAmine). With regards to the thermodynamic equilibrium properties, vapor-liquid phase equilibrium diagrams, vaporization enthalpies and vapor pressures were studied. Figures 2, 3 and 4 give the phase equilibrium diagrams, vaporization enthalpies and vapor pressures respectively.

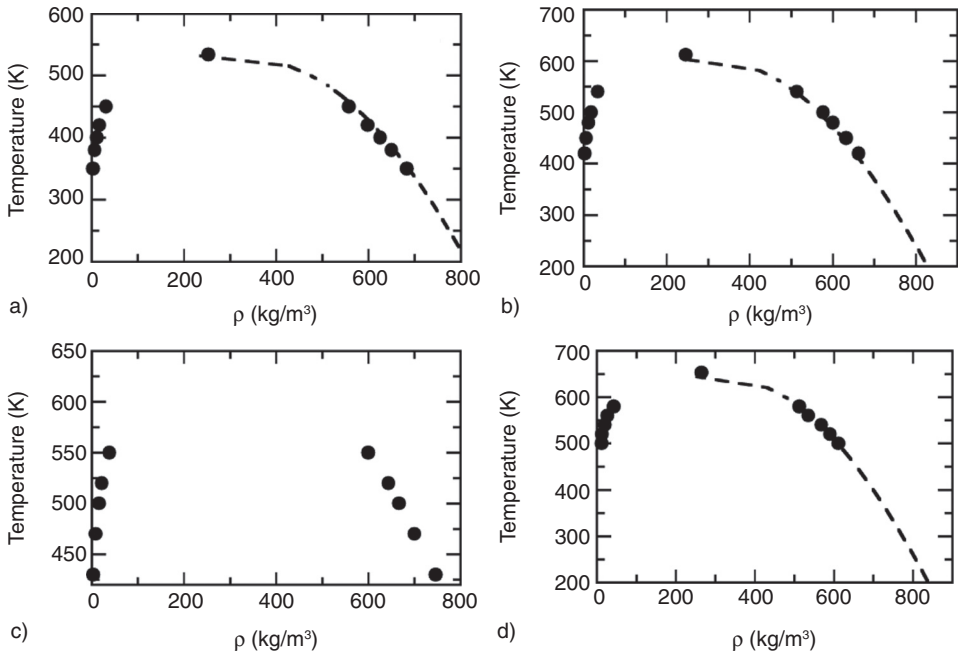


Figure 2

Liquid-vapor phase equilibrium diagrams. a) *n*-ButylAmine, b) Di-*n*-ButylAmine, c) 1,4-ButaneDiAmine, d) Tri-*n*-ButylAmine. The circles represent the simulation results while the dashed line corresponds to experimental data [39, 40].

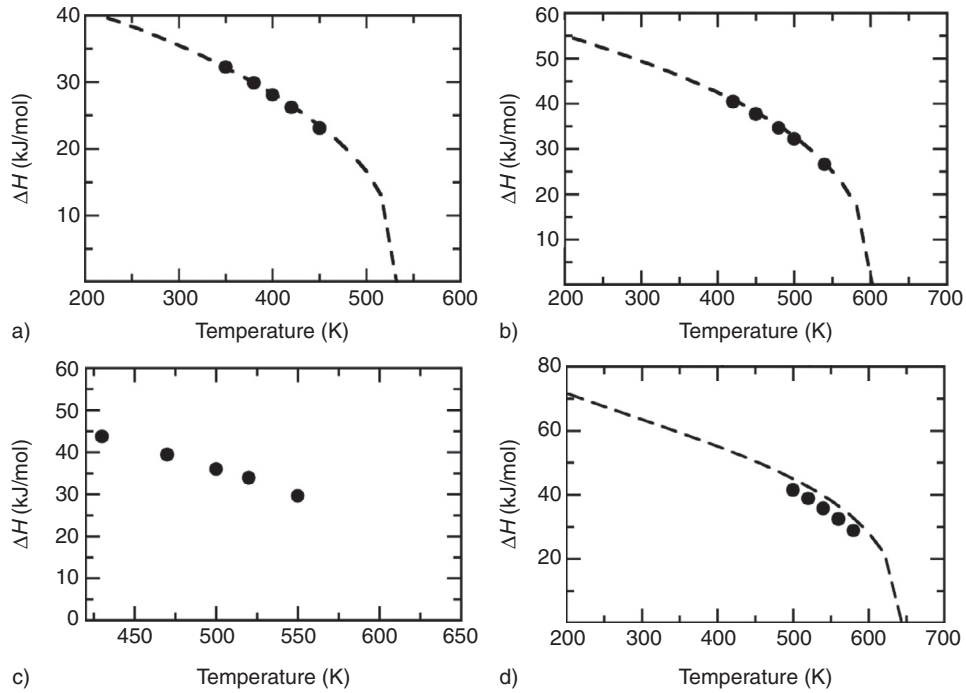


Figure 3

Vaporization enthalpies. a) *n*-ButylAmine, b) Di-*n*-ButylAmine, c) 1,4-ButaneDiAmine, d) Tri-*n*-ButylAmine. The circles represent the simulation results while the dashed line corresponds to experimental data [39, 40].

Nearly all the experimental information was taken from the DIPPR [39] and NIST [40] databases. It should be noted that some of these values are based on predictions, this is the case of both vaporization enthalpies and vapor pressures for tri-*n*-ButylAmine based on the Clapeyron equation and Riedel's method with numerical uncertainties of 5% for both of them. The associated experimental uncertainties for other molecules are around 1% for liquid densities ($\rho_L$), 5% for vaporization enthalpies ($\Delta H$) and 5% for vapor pressures ($P_v$). No experimental data were found for 1,4-ButaneDiAmine.

Absolute Average Deviations (AAD $= \frac{|X^{exp} - X^{calc}|}{X^{exp}} 100\%$) were calculated for all the studied molecules obtaining: 1% for $\rho_L$, 3.5% for $\Delta H$ and 9% for $P_v$.

### 3.1 Critical Points and Normal Boiling Points

The critical temperature ($T_c$) and critical density ($\rho_c$) were calculated from the scaling law defined by Equation (14) and the law of rectilinear diameters (*Eq. 15*).

$$\rho_L - \rho_V = A(T_c - T)^{\beta^*} \tag{14}$$

$$\frac{\rho_L + \rho_V}{2} = \rho_c + B(T_c - T) \tag{15}$$

where $\rho_L$ and $\rho_V$ correspond to the coexisting liquid and vapor densities, $\beta^*$ is a characteristic universal exponent (for this work $\beta^* = 0.325$ [29]), $A$ and $B$ are adjustable parameters.

Normal boiling points ($T_b$) have been calculated by means of the Clausius-Clapeyron equation. Table 7 summarizes the obtained values.

Nearly all the comparisons were done with experimental information [39], except for the values with star superscripts (*), which correspond to predictions [39] where the associated uncertainties are stated to vary between 3% and 10%.

From Table 7, it is possible to see how the force field is able to reproduce the correct trend, *i.e.*, the increasing on both the normal boiling point and critical temperature as the number of carbons increases from primary to tertiary amines. Considering the associated uncertainties on the experimental data, for all the studied molecules, the obtained simulation results are in excellent agreement with them, which ratifies the accuracy of the AUA4 force field for amines.

### 3.2 Excess Enthalpies

In 2004, one of the proposed problems for the second fluid simulation challenge [41] was to determine the

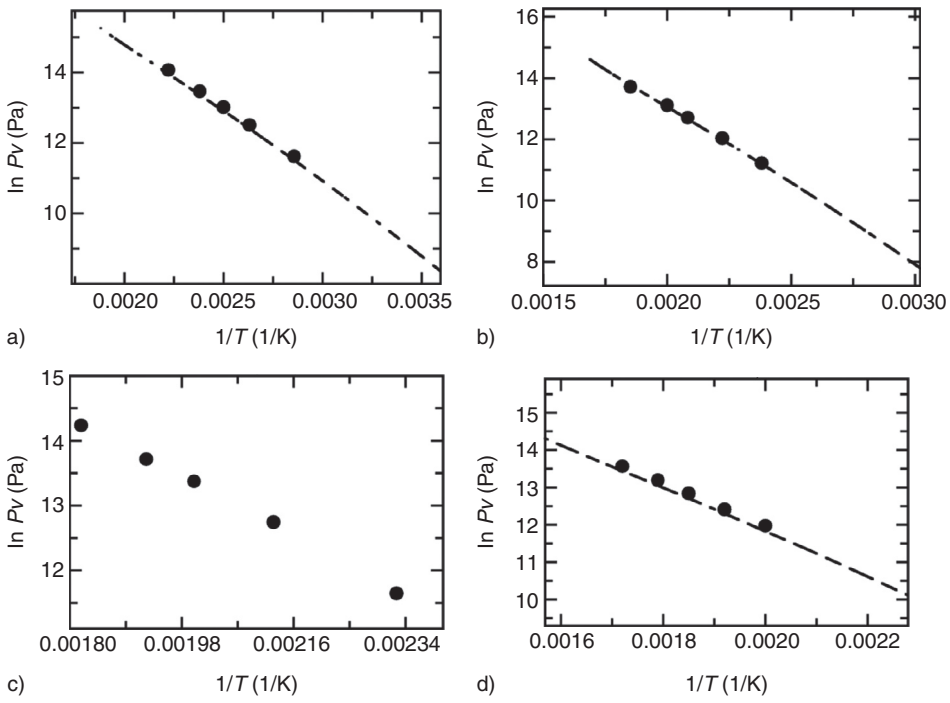


Figure 4

Vapor pressures. a) *n*-ButylAmine, b) Di-*n*-ButylAmine, c) 1,4-ButaneDiAmine, d) Tri-*n*-ButylAmine. The circles represent the simulation results while the dashed line corresponds to experimental data [39, 40].

TABLE 7

Critical coordinates and normal boiling points, comparison between experimental or predicted values and calculations using the AUA4 force field for amines

| Molecule | $T_c$ (K) | | $\rho_c$ (kg/m$^3$) | | $T_b$ (K) | |
|---|---|---|---|---|---|---|
| | Exp. | Sim. | Exp. | Sim. | Exp. | Sim. |
| BA | $532_5$ | $534_3$ | *$236_{11}$ | $253_7$ | $351_4$ | $347_5$ |
| DBA | $602.3_5$ | $612_6$ | *$252_{12}$ | $246_8$ | $432_5$ | $430_6$ |
| TBA | $644_{30}$ | $653_8$ | *$252_{60}$ | $265_8$ | $487_5$ | $480_6$ |
| BDA | na | $638_6$ | na | $292_8$ | na | $425_8$ |

* DIPPR predicted values. Experimental values taken from DIPPR and NIST databases [39, 40], na = not available. BA = *n*-ButylAmine, DBA = Di-*n*-ButylAmine, TBA = Tri-*n*-ButylAmine, BDA = 1,4-ButaneDiAmine. The subscripts give the statistical uncertainties of the last digit(s).

excess properties of *n*-ButylAmine + water and *n*-ButylAmine + *n*-heptane. In this competition, two different force fields were presented. The first one was an all atom potential proposed by Dai *et al.* [42] and the second was the work that has already been mentioned proposed by Boutard *et al.* [20] based on a AUA approach. In the first case, calculations were done using molecular dynamics, while in the second one Monte Carlo simulations were used. One interesting characteristics of these mixtures is related to the fact that the excess enthalpies have a different sign in both systems, *i.e.* when *n*-ButylAmine is mixed with water a negative sign of the excess enthalpy is expected, while with *n*-heptane a positive excess enthalpy is observed. Both models managed to get the correct behavior for the *n*-ButylAmine + *n*-heptane system, but unfortunately neither of them managed to obtain the right behavior for *n*-ButylAmine + water mixture, *i.e.*, for this system, these two models predicted a positive sign for the excess enthalpies.

In view of these results, we felt it was important to check the ability of our new AUA4 force field to predict excess enthalpies. As can be inferred from the previous paragraph, determining these kind of properties is considered to be a challenge from a molecular simulation point of view due to the fact that the interactions between unlike molecules are actually difficult to capture, especially in the case of non-polarizable force fields. In addition, given that for the $CO_2$ processes mentioned in the introduction, amines are always used in aqueous solutions, the intermolecular potentials need to capture the correct mixture behavior. In other words, the excess enthalpies are important because they reflect the difference of molecular interactions between the pure components and the unlike components. If this property is not well predicted then the Henry constants will probably also be incorrect or unreliable because the interactions in the solvent are poorly described.

Figure 5 shows a comparison between our excess enthalpy predictions and the experimental information [43-45] taken from the DETHERM database [46] for the *n*-ButylAmine + water system. It is worth pointing out that differences between experimental values can be found. Although all of them show the same qualitative behavior, there are significant discrepancies. As can be seen from this figure, our force field is able to reproduce the correct behavior. It should be noted that both the water and the *n*-ButylAmine models are non-polarizable without any adjustment for this mixture. From a quantitative point of view, our results are in excellent agreement with the experimental values of Mato and Berrueta [45]. With regards to the *n*-heptane + *n*-ButylAmine mixture, as can be seen in Figure 6, our force field predictions overestimate the excess enthalpies but are able to reproduce the order of magnitude correctly. Nevertheless, from a qualitative point of view, the positive deviation from ideality is well reproduced which in itself is a significant achievement.

### 3.3 Surface Tensions

Figure 7 shows experimental (DIPPR) and calculated liquid-vapor surface tensions for *n*-ButylAmine for temperatures ranging from 300 K to 475 K.

Results using both IK and TA methods are in good agreement between themselves as well as with experiments, although average deviations are of 10.7% for the IK method and 8.4% for the TA method. This result is particularly remarkable if we recall that surface tension values were not used to parameterize this force field, and it thus highlights its transferability to other properties.

Figure 8 shows the density profile along the $z$-axis (normal to the interface) at 400 K for the same *n*-ButylAmine system. It is possible to fit such a profile to the hyperbolic tangent function given by:

$$\rho(z) = \frac{1}{2}(\rho_l + \rho_v) - \frac{1}{2}(\rho_l - \rho_v)\tanh\left(\frac{2(z - z_0)}{d}\right) \quad (16)$$

giving a direct estimate of the liquid ($\rho_l$) and vapor ($\rho_v$) densities and an approximate idea of the interface thickness $d$. The parameter $z_0$ gives the position of the

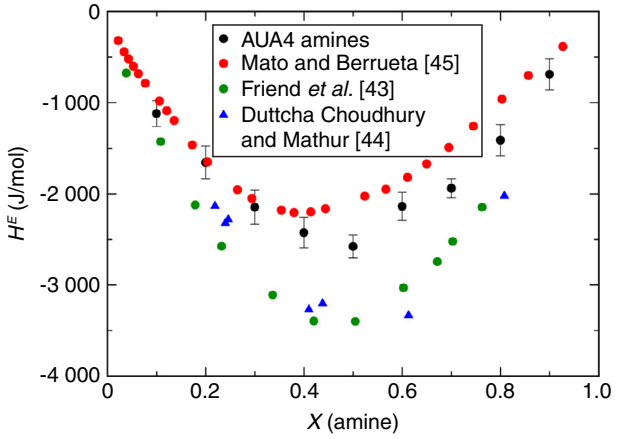


Figure 5

Excess enthalpies. *n*-ButylAmine + water. Black circles correspond to the simulation results, while other symbols are experimental values [43-45]. The dashed line is just a guide for the eye.

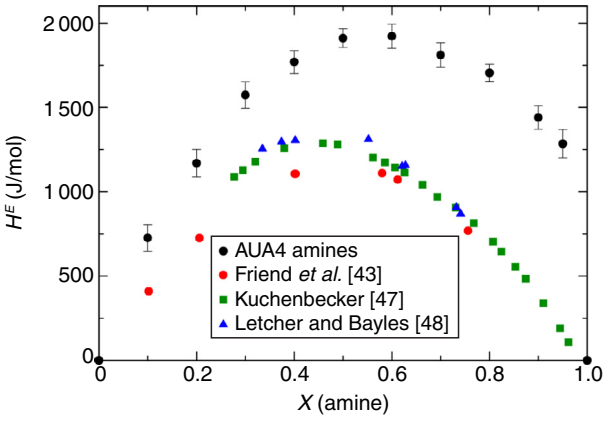


Figure 6

Excess enthalpies. *n*-ButylAmine + *n*-heptane. Black circles correspond to the simulation results, while other symbols are experimental values [43, 47, 48].

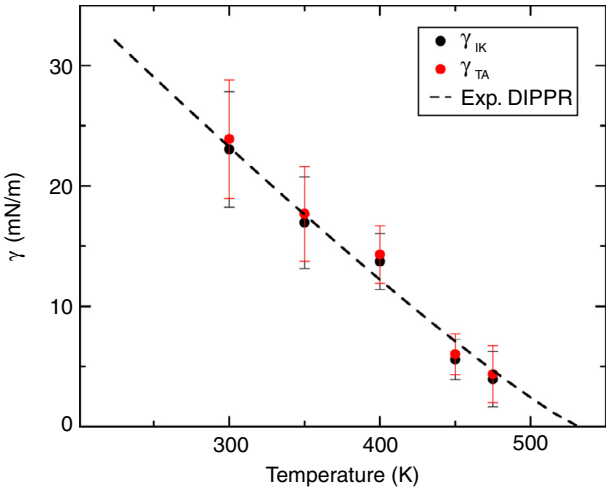


Figure 7

Surface tensions of *n*-ButylAmine. The circles give the AUA4 simulation data and the line corresponds to the experimental data from the DIPPR database [39].

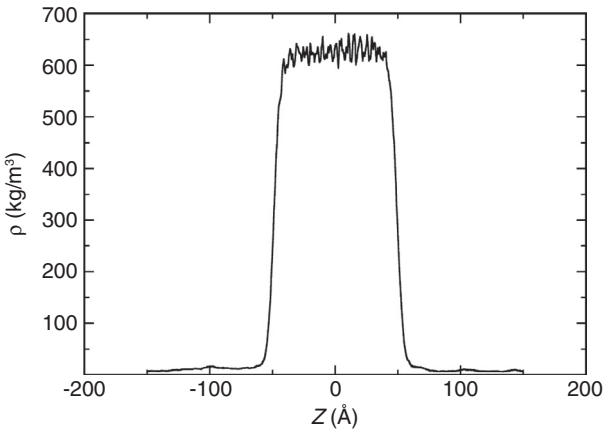


Figure 8

Density profile along the *z*-axis for liquid-vapor equilibrium of *n*-ButylAmine at 400 K.

interface. When fitting the density profile given in Figure 8, values of 626.4 and 9.9 kg/m$^3$ were found for $\rho_l$ and $\rho_v$ which are in excellent agreement with the ones obtained using the Gibbs ensemble technique (625.6 and 10.9 kg/m$^3$). An interface thickness of 10.1 Å was also obtained.

### 3.4 Henry Constants

It is well known that $CO_2$ sorption by means of amine solvents involves chemical reactions. Nevertheless, in this work these reactions are not going to be considered and only the physical solubility through the Henry constant, will be calculated. In order to do that the $N_2O$ analogy will be used.

In addition, the Henry constants of $N_2$ will also be calculated. Since we have demonstrated in the previous section that our force field successfully reproduces the behavior of the *n*-ButylAmine + water mixture we will predict the Henry constants in this mixture.

We have calculated the physical Henry constants of ($N_2O$) and ($N_2$) in an aqueous solution of *n*-ButylAmine. Simulations were carried out in the isothermal-isobaric ensemble (NPT) at one atmosphere and simulating two different temperatures 303 K and 313 K respectively. 32 molecules of *n*-ButylAmine and 368 of water were used which corresponds to a molar concentration of amine of 8%.

In order to determine the Henry constants, we employed the Widom test particle method in simulations of 550 million MCS. Table 8 summarizes the obtained results using the AUA4 force field for amines. Unfortunately experimental Henry constants are only available for alkanolamines, but not for monofunctional amines. From the table, it can be seen that the Henry constant increases as temperature increases for both gases, we also observe the small solubility of $N_2$ compared with $N_2O$.

### 3.5 Transport Properties: Viscosity Coefficients

Molecular dynamic simulations were carried out at five different temperatures and atmospheric pressure. In order to calculate the viscosity coefficients, both the Green-Kubo and the Einstein formalisms were employed, obtaining equivalent numerical values within the statistical uncertainties. Figure 9 shows a comparison between the experimental (grey filled circles) and the simulated (black filled squares) viscosity coefficients for the studied molecules given in centipoises (cP). Four amine molecules were studied, namely: *n*-ButylAmine, Di-*n*-ButylAmine, Tri-*n*-ButylAmine and 1,4-ButaneDiAmine. Experimental information were taken directly from the work of Shah *et al.* [49], however, no experimental information was found for 1,4-ButaneDiAmine. We found absolute average deviations of 20%, 8% and 10%, for *n*-ButylAmine, Di-*n*-ButylAmine and Tri-*n*-ButylAmine respectively. It is important to mention that for primary amines the results are consistent with the transferability of the AUA4 force field for hydrocarbons and with previous calculations for short amines such as *n*-PropylAmine [16]. For Di-*n* and Tri-*n*-ButylAmine results are in very good agreement with the experimental data.

TABLE 8
Henry constants for ($N_2O$) and ($N_2$) in an aqueous solution of *n*-ButylAmine (8% mol), $P = 1$ atm

| Gas | Temperature (K) | $K_H$ (MPa) |
|---|---|---|
| $N_2O$ | 303 | 168.3 |
| | 313 | 206.1 |
| $N_2$ | 303 | 4 318.4 |
| | 313 | 4 948.1 |

## 3.6 Radial Distribution Functions

Molecular simulation allows us to explore the structure of matter through the radial distribution function ($g_{XY}$). This function tells us the number of neighboring atoms ($Y$) around a particular one ($X$) in a defined volume. If atoms $X$ and $Y$ belong to different molecules, we talk about an intermolecular radial distribution function, on the other hand, if $X$ and $Y$ belong to the same molecule, we can define a histrogram of distances in order to find out about the possible molecule conformations.

In the following a comparison between the liquid structure of primary, secondary and tertiary amines is presented. To the best of our knowledge, there is no available experimental information to compare with, except for methylamine which was already studied in previous works [16]. Hence, the discussion will be merely qualitative.

### 3.6.1 Intermolecular $g_{XY}$

Figure 10 shows the radial distribution functions at atmospheric pressure for a) the primary amine *n*-ButylAmine at 270 K, b) the secondary amine Di-MethylAmine at 250 K, c) the tertiary amine Tri-MethylAmine at 298 K, and d) the multifunctional amine 1,4-ButaneDiAmine (BDA) at 313 K. For *n*-ButylAmine a), a similar behavior to the one presented by methylamine in a previous work was found [16]. That is to say, two peaks in the $g_{NH}$ are found, the first one at ~2.4 Å which might indicate the presence of a hydrogen bond with a coordination number of 1 and the second peak around ~3.6 Å that corresponds to the second solvation shell. In addition, a well defined peak can be seen around ~3.4 Å for the $g_{NN}$ that yields a coordination number of 4. For Di-MethylAmine b), maxima are located in the same positions as for

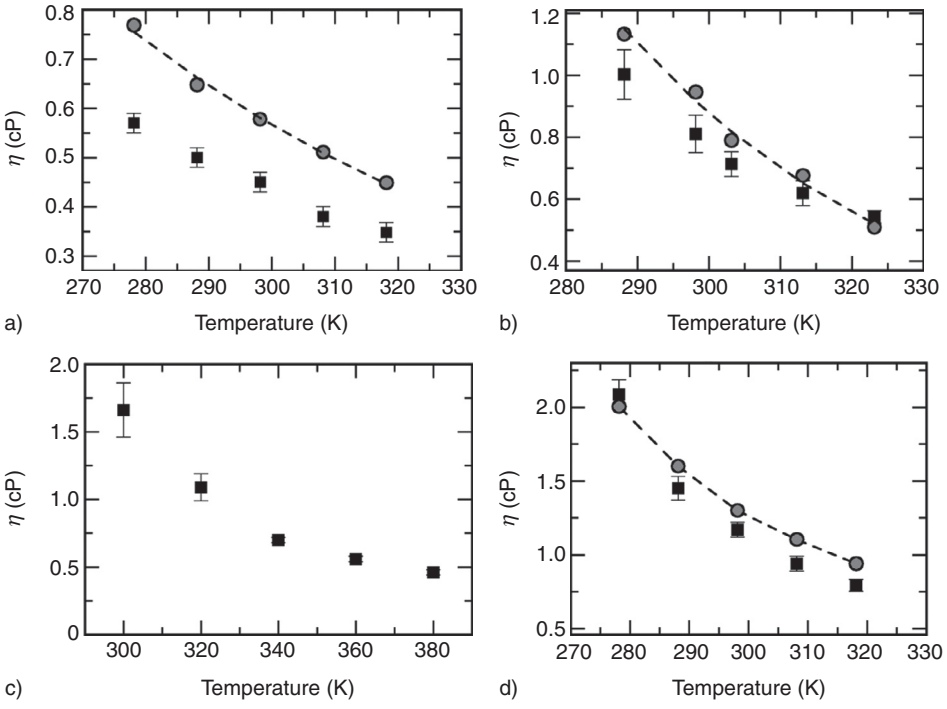


Figure 9

Shear viscosity as a function of temperature. Grey filled circles correspond to experimental data and black filled squares to simulation results. a) *n*-ButylAmine, b) Di-*n*-ButylAmine, c) 1,4-ButaneDiAmine, d) Tri-*n*-ButylAmine. The dashed line is just a guide for the eye.

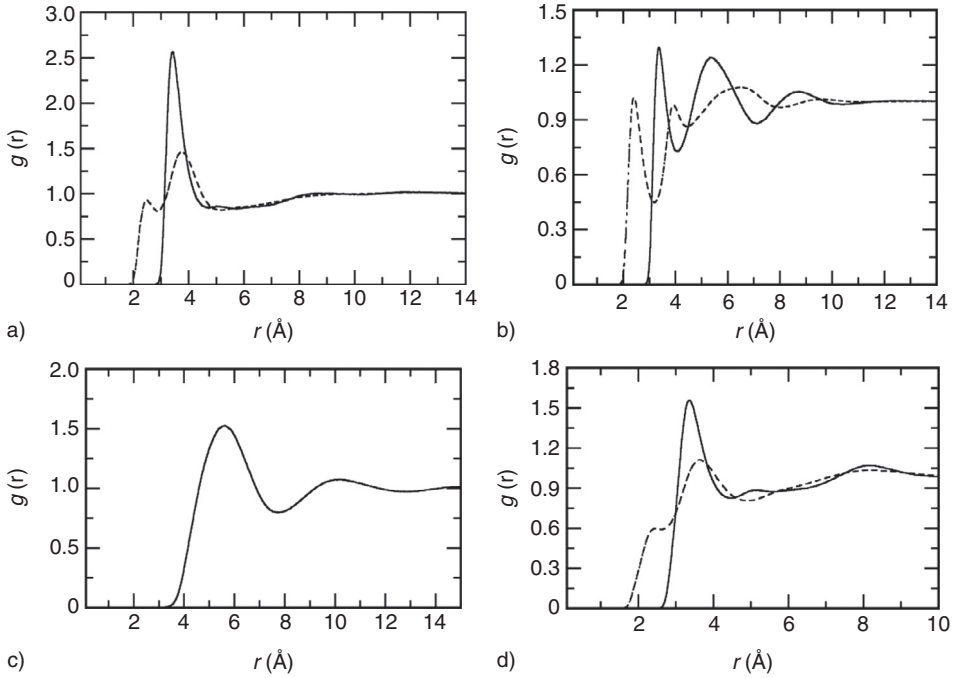


Figure 10

Amine intermolecular radial distribution functions. a) *n*-ButylAmine 270 K, b) Di-MethylAmine 250 K, c) Tri-MethylAmine 298 K, d) 1,4-ButaneDiAmine 313 K. For all cases solid and dashed lines correspond to $g_{NN}$ and $g_{NH}$ respectively.

*n*-ButylAmine, but are smaller in magnitude. Integration of the first peaks for $g_{NH}$ and $g_{NN}$ yields coordination numbers of ~0.8 and ~3.8 respectively. For Tri-Methyl-Amine c), it is possible to identify a first solvation shell which is represented by the well defined peak at ~5.3 Å yielding a coordination number of 3.6. It is important to mention that in our model this molecule has no hydrogen so that it does not have the possibility to form hydrogen bonds, at least as a pure component. This might be considered as a disadvantage of the AUA approach compared to an all atom, nevertheless, hydrogen bond formation was also not found for tertiary components according to the results presented by Rizzo and Jorgensen [18] using the OPLS-AA model. This could be expected because the nitrogen in tertiary amines is well hidden by the three bonded carbons and there is probably no significant interaction with the hydrogens belonging to the hydrocarbonated part of the molecule which in addition are not charged. With regards to 1,4-ButaneDiAmine, see Figure 10d, a similar behavior to that of *n*-ButylAmine can be observed.

It is important to mention that intramolecular interactions can play an interesting role in bifunctional molecules and in the next section, we center our discussion on this aspect.

### 3.6.2 Intramolecular Interactions: Multifunctional Amines

An interesting feature involving multifunctional amines is the ability to form intramolecular hydrogen bonds. It is known form previous works based on both *ab-initio* calculations [50, 51] and experiments [51, 52] that for 1,2-EthaneDiAmine (EDA) in the gas phase the most stable conformation presents an intramolecular hydrogen bond and corresponds to the gauche conformation (with respect to the C-C bond). This result has been also recently reported by Bryantsev *et al.* [53] through a computational conformational study that included bifunctional aliphatic amines in the gas phase and in aqueous solutions. Batista de Carvalho *et al.* [51] have carried out Raman spectroscopy experiments on EDA in the solid state, pure liquid and aqueous solutions. They have found that the most stable conformer in the solid and in the gas phase corresponds to the gauche conformation while in aqueous solutions the trans conformation was the preferred one, followed by a very small population

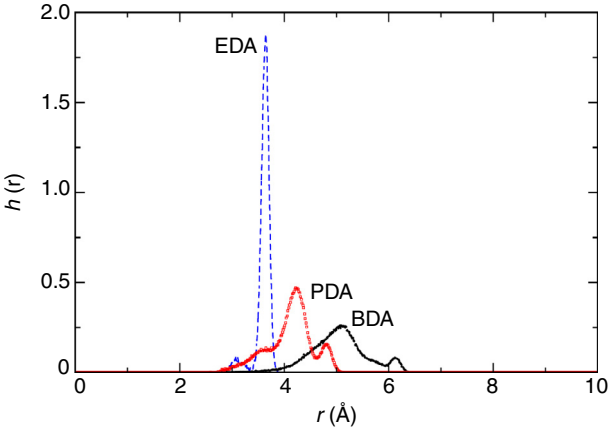


Figure 11

Histograms of the N-N intramolecular distances (380 K and atmospheric pressure) for 1,2-EthaneDiAmine (EDA), 1,3-PropaneDiAmine (PDA) and 1,4-ButaneDiAmine (BDA).

in the gauche conformation. Such behavior has been also found by Bryantsev *et al.* [53] using Density Functional Theory (DFT) and by Gubskaya and Kusalik [54] performing molecular dynamics in pure liquid EDA. Concerning 1,3-PropaneDiAmine (PDA) and 1,4-ButaneDiAmine (BDA), Bryantsev *et al.* [53] have also found by means of DFT that the trans conformation is favored for PDA and BDA and there is no intramolecular hydrogen bond formation. However for these last results, there is no experimental data that confirm their results.

Histograms of the nitrogen-nitrogen intramolecular distances are shown in Figure 11 for the three diamines (1,2-EthaneDiAmine, 1,3-PropaneDiAmine and 1,4-ButaneDiAmine) at 380 K and atmospheric pressure. For 1,2-EthaneDiAmine, the distribution exhibits two distinct peaks: the first one (~3 Å) corresponds to a gauche conformation of the N-$CH_2$-$CH_2$-N dihedral angle, which favors the formation of an intramolecular hydrogen bond. About 7% of the molecules in the bulk are found in a gauche conformation. The second peak (~3.6 Å) corresponds to a trans conformation of the molecule. For 1,3-PropaneDiAmine and 1,4-ButaneDiAmine, the main peaks of the distribution are located around 4.2 and 5.3 Å respectively, which suggests the absence of intramolecular hydrogen bond for both molecules. The last peaks of these distributions (~6.1 and ~4.8 Å respectively) correspond to a geometry in which all the dihedral angles of the molecule are in trans conformation. Integration shows that about 11% and 8% of the molecules in the bulk adopt a trans conformation for PDA and BDA respectively.

## CONCLUSIONS

In this molecular simulation work, predictions of different thermophysical properties have been shown based on our recently proposed AUA4 force field for primary, secondary and tertiary amines. Using both molecular dynamics and MC methods, we have taken advantage of several molecular simulation techniques such as: Gibbs ensemble, Widom test particle insertion, Einstein and Green Kubo formalisms, Irving-Kirkwood and Test-Area approaches. The properties we have investigated in this work are: liquid-vapor phase diagrams, vaporization enthalpies, vapor pressures, critical densities, critical temperatures, normal boiling points, surface tensions, excess enthalpies, Henry constants and viscosity coefficients. We can conclude that:

- the very good to excellent agreement with experiments obtained in the studied properties ratifies the predictive capability of our force field. Including this work, up to now, this force field for amines has been tested on a total of 25 different amines. Besides all the previously studied properties, we have included here new calculations on surface tensions and Henry constants. To our knowledge, none of the currently available force fields has been tested on so many properties as this one;
- for the thermodynamic equilibrium properties we have obtained in general global average deviations from experiments of 1% for liquid densities, 3.5% for vaporization enthalpies and 9% for vapor pressures. Estimations of the normal boiling points were predicted with less than 1% error as compared with experimental values;
- concerning the viscosity coefficients, a very good accuracy is obtained for secondary and tertiary amines and a fair good agreement for short linear primary amines. For the latter case (short linear primary amines), it should be noted that these deviations are of the same magnitude as the ones obtained for short linear alkanes;
- our force field is able to correctly reproduce the sign of the excess enthalpy for *n*-ButylAmine when this molecule is mixed with water and *n*-heptane, obtaining negative excess values for the first case and positive ones when mixed with *n*-heptane;
- Henry constants of $N_2O$ and $N_2$ were also calculated in a mixture of *n*-ButylAmine + water. However, to our knowledge, no experimental information is available to compare with;

– for surface tensions the results derived from the two different investigated methods were equivalent obtaining global average deviations of around 10%. In the same manner, the viscosity coefficients obtained by both the Green Kubo and the Einstein methodologies were consistent. Finally, additional results on the liquid structure were presented and compared with previous works mostly based on simulations. For the case of intramolecular conformations it was possible to compare our simulation results with available experimental data for 1,2-EthaneDiAmine but not for longer diamines.

## ACKNOWLEDGMENTS

G.A. Orozco acknowledges IFP Energies nouvelles for his PhD grant. The authors would like to thank Dr. Bernard Rousseau for the use of the NEWTON code. This work was performed using HPC resources from GENCI-CCRT/CINES (Grant 2012-x2012096349).

## REFERENCES

1 Toxvaerd S. (1990) Molecular dynamics calculation of the equation of state of alkanes, *J. Chem. Phys.* **93**, 4290-4295.

2 Ungerer P., Beauvais C., Delhommelle J., Boutin A., Rousseau B., Fuchs A.H. (2000) Optimization of the anisotropic united atoms intermolecular potential for *n*-alkanes, *J. Chem. Phys.* **112**, 5499-5510.

3 Delhommelle J., Tschirwitz C., Ungerer P., Granucci G., Millie P., Pattou D., Fuchs A.H. (2000) Derivation of an optimized potential model for phase equilibria (OPPE) for sulfides and thiols, *J. Chem. Phys.* **104**, 4745-4753.

4 Bourasseau E., Ungerer P., Boutin A. (2002) A general and efficient Monte Carlo method for sampling intramolecular degrees of freedom of branched and cyclic molecules, *J. Phys. Chem. B* **112**, 5483-5491.

5 Bourasseau E., Haboudou M., Boutin A., Fuchs A.H., Ungerer P. (2003) New optimization method for intermolecular potentials: Optimization of a new anisotropic united atoms potential for olefins: Prediction of equilibrium properties, *J. Chem. Phys.* **118**, 3020-3034.

6 Contreras-Camacho R.O., Ungerer P., Boutin A., Mackie A.D. (2004) Optimized intermolecular potential for aromatic hydrocarbons based on anisotropic united atoms. 1. Benzene, *J. Phys. Chem. B* **108**, 14109-14114.

7 Ahunbay M.G., Pérez-Pellitero J., Contreras-Camacho R. O., Teuler J.M., Ungerer P., Mackie A.D., Lachet V. (2005) Optimized intermolecular potential for aromatic hydrocarbons based on anisotropic united atoms. III. Polyaromatic and naphthenoaromatic hydrocarbons, *J. Phys. Chem. B* **109**, 2970-2976.

8 Bonnaud P., Nieto-Draghi C., Ungerer P. (2007) Anisotropic united atom model including the electrostatic interactions of methylbenzenes. I. Thermodynamic and structural properties, *J. Phys. Chem. C* **111**, 3730-3741.

9 Pérez-Pellitero J., Ungerer P., Mackie A.D. (2007) An anisotropic united atoms (AUA) potential for thiophenes, *J. Phys. Chem.* **111**, 4460-4466.

10 Pérez-Pellitero J., Bourasseau E., Demachy I., Ridard I., Ungerer P., Mackie A.D. (2008) Anisotropic united-atoms (AUA) potential for alcohols, *J. Phys. Chem. B* **112**, 9853-9863.

11 Ferrando N., Lachet V., Teuler J.M., Boutin A. (2009) Transferable force field for alcohols and polyalcohols, *J. Phys. Chem. B* **113**, 5985-5995.

12 Creton B., de Bruin T., Lachet V., Nieto-Draghi C. (2010) Extension of a charged anisotropic united atoms model to polycyclic aromatic compounds, *J. Phys. Chem. B* **114**, 6522-6430.

13 Ferrando N., Lachet V., Boutin A. (2009) Monte Carlo simulations of mixtures involving ketones and aldehydes by a direct bubble pressure calculation, *J. Phys. Chem. B* **114**, 8680-8688.

14 Ferrando N., Lachet V., Boutin A. (2011) A transferable force field to predict phase equilibria and surface tension of ethers and glycol ethers, *J. Phys. Chem. B* **15**, 10654-10664.

15 Ferrando N., Lachet V., Boutin A. (2012) Transferable force field for carboxylate esters: application to fatty acid methylic ester phase equilibria prediction, *J. Phys. Chem. B* **116**, 3239-3248.

16 Orozco G.A., Nieto-Draghi C., Mackie A.D., Lachet V. (2011) Transferable force field for equilibrium and transport properties in linear and branched monofunctional and multifunctional amines. I. Primary amines. *J. Phys. Chem. B* **115**, 14617-14625.

17 Orozco G.A., Nieto-Draghi C., Mackie A.D., Lachet V. (2012) Transferable force field for equilibrium and transport properties in linear, branched, and bifunctional amines II. Secondary and tertiary amines, *J. Phys. Chem. B* **116**, 6193-6202.

18 Rizzo R.C., Jorgensen W.L. (1999) OPLS all atom model for amines: Resolution of the amine hydration problem, *J. Am. Chem. Soc.* **121**, 4827-4836.

19 Wick C.D., Stubbs J.M., Neeraj R., Siepmann J.I. (2005) Transferable potentials for phase equilibria. 7. Primary, secondary, and tertiary amines, nitroalkanes and nitrobenzene, nitriles, amides, pyridine, and pyrimidine, *J. Phys. Chem. B* **109**, 18974-18982.

20 Boutard Y., Ungerer P., Teuler J.M., Ahunbay M., Sabater S., Pérez-Pellitero J., Mackie A.D., Bourasseau E. (2005) Extension of the anisotropic united atoms intermolecular potential to amines, amides and alkanols. Application to the problems of the 2004 fluid simulation challenge, *Fluid Phase Equilib.* **236**, 25-41.

21 Ungerer P., Tavitian B., Boutin A. (2005) *Applications of molecular simulation in the Oil and Gas Industry*, Technip, Paris, p. 267.

22 Chen K.H., Lii J.H., Fan Y., Allinger N.L. (2007) Molecular mechanics (MM4) study of amines, *J. Comput. Chem.* **28**, 2391-2412.

23 Abascal J.F.L., Vega C. (2005) A general purpose model for the condensed phases of water: TIP4P/2005, *J. Chem. Phys.* **123**, 234505-234516.

24 Vega C., Abascal L.F. (2011) Simulating water with rigid non-polarizable models: a general perspective, *Phys. Chem. Chem. Phys.* **13**, 19663-19688.

25 Lachet V., Creton B., de Bruin T., Bourasseau E., Desbiens N., Wilhelmsen O., Hammer M. (2012) Equilibrium and transport properties of $CO_2$ + $N_2O$ and $CO_2$ + NO mixtures: Molecular simulation and equation of state modelling study, *Fluid Phase Equilib.* **322**, 66-78.

26 Delhommelle J. (2000) *PhD Thesis*, Université Paris-Sud, Orsay, France.

27 Van-Oanh N.T., Houriez C., Rousseau B. (2010) Viscosity of the 1-ethyl-3-methylimidazolium bis(trifluoromethylsulfonyl)imide ionic liquid from equilibrium and nonequilibrium molecular dynamics, *Phys. Chem. Chem. Phys.* **12**, 930-936.

28 Panagiotopoulos A.Z. (1987) Direct determination of phase coexistence properties of fluids by Monte Carlo simulation in a new ensemble, *Molec. Phys.* **61**, 813-826.

29 Frenkel D., Smit B. (2002) *Understanding molecular simulations*, Academic Press, New York, p. 201.

30 Andersen H. (1983) Rattle: A velocity version of the Shake algorithm for molecular dynamics calculations, *J. Comp. Phys.* **52**, 24-34.

31 Widom B. (1963) Some topics in the theory of fluids, *J. Chem. Phys.* **39**, 2808-2812.

32 Biscay F., Ghoufi A., Lachet V., Malfreyt P. (2009) Monte Carlo calculation of the methane-water interfacial tension at high pressures, *J. Chem. Phys.* **131**, 124707.

33 Trokhymchuk A., Alejandre J. (1999) Computer simulations of liquid/vapor interface in Lennard-Jones fluids: Some questions and answers, *J. Chem. Phys.* **111**, 8510-8523.

34 Orea P., Lopez-Lemus J., Alejandre J. (2005) Oscillatory surface tension due to finite-size effects, *J. Chem. Phys.* **123**, 114702.

35 Biscay F., Ghoufi A., Lachet V., Malfreyt P.J. (2009) Monte Carlo simulations of the pressure dependence of the water-acid gas interfacial tensions, *J. Phys. Chem. B* **113**, 14277-14290.

36 Biscay F., Ghoufi A., Goujon F., Lachet V., Malfreyt P. (2009) Calculation of the surface tension from Monte Carlo simulations: Does the model impact on the finite-size effects? *J. Chem. Phys.* **130**, 184710.

37 Irving J.H., Kirkwood J.G. (1950) The statistical mechanical theory of transport processes. IV. The equations of hydrodynamics, *J. Chem. Phys.* **18**, 817-829.

38 Gloor G.J., Jackson G., Blas F.J., de Miguel E. (2005) Test-area simulation method for the direct determination of the interfacial tension of systems with continuous or discontinuous potentials, *J. Chem. Phys.* **123**, 134703.

39 DIPPR 801 Thermophysical property database, DIADEM professional, 2008.

40 http://cccbdb.nist.gov.

41 Case F., Chaka A., Friend D.G., Frurip D., Golab J., Gordon P., Johnson R., Kolar P., Moore J., Mountain R.D., et al. (2005) The second industrial fluid properties simulation challenge, *Fluid Phase Equilib.* **236**, 1-14.

42 Dai J.X., Wu C.J., Bao X.G., Sun H. (2005) Prediction of the heat of mixing for binary fluids using molecular dynamics simulation, *Fluid Phase Equilib.* **236**, 78-85.

43 Friend D.G., Frurip D.J., Lemmon E.W., Morrison R.E., Olson J.D., Wilson L.C. (2005) Establishing benchmarks for the second industrial fluids simulation challenge, *Fluid Phase Equilib.* **236**, 15-24.

44 Duttcha Choudhury M.K., Mathur H.B. (1974) Heats of mixing of *n*-butyl amine - water and *n*-butyl amine - alcohol systems, *J. Chem. Eng. Data* **16**, 145-147.

45 Mato F., Berrueta J. (1978) Heat of mixing of exothermic systems, *An. Quim.* **74**, 1290-1293.

46 Detherm Thermophysical Properties of Pure Substances and Mixtures (2007) Dechema, Frankfurt am, Main.

47 Kuchenbecker D. (1980) *PhD Thesis*, Leipzig.

48 Letcher T.M., Bayles J.W. (1971) Thermodynamics of some binary liquid mixtures containing aliphatic amines, *J. Chem. Eng. Data* **16**, 266-271.

49 Shah J., Dewitt J., Stoops C. (1969) Viscosity-temperature correlation for liquid aliphatic amines, *J. Chem. Eng. Data* **14**, 333-335.

50 Chang Y.P., Su. T.M., Li T.W., Chao I. (1997) Intramolecular hydrogen bonding, gauche interactions, and thermodynamic functions of 1,2-ethanediamine, 1,2-ethanediol, and 2-aminoethanol: A global conformational analysis, *J. Phys. Chem. A* **101**, 6107-6117.

51 Batista de Carvalho L.A.E., Lourenco L.E., Marques M.P. M. (1999) Conformational study of 1,2-diaminoethane by combined *ab initio* MO calculations and Raman spectroscopy, *J. Mol. Struct.* **482-483**, 639-646.

52 Marstokk K.M., Mollendal H. (1978) Microwave spectrum, conformational equilibrium, intramolecular hydrogen bonding, inversion tunneling, dipole moments, and centrifugal distortion of ethylenediamine, *J. Mol. Struct.* **49**, 221-237.

53 Bryantsev V.S., Diallo M.S., Goddard W.A.I.I.I. (2007) pKa calculations of aliphatic amines, diamines, and aminoamides *via* density functional theory with a Poisson-Boltzmann continuum solvent model, *J. Phys. Chem. A* **111**, 4422-4430.

54 Gubskaya A.V., Kusalik P.K. (2004) Molecular dynamics simulation study of ethylene glycol, ethylenediamine and 2-aminoethanol. 1. The local structure in pure liquids, *J. Phys. Chem. B* **108**, 7151-164.


*Manuscript accepted in April 2013*
*Published online in Jamuary 2014*